International Journal of Engineering & Technology, 7 (3) (2018) 1145-1149

International Journal of Engineering & Technology

Website: www.sciencepubco.com/index.php/IJET
doi: 10.14419/ijet.v7i3.12605
Research paper



Evaluation of residual stresses in multipass dissimilar butt-welded of SS316L to Inconel625 using FEA

Harinadh Vemanaboina [1] *, G. Edison [1], Suresh Akella [2]

[1] *SMEC, Vellore Institute of Technology, Vellore, Tamilnadu, India*
[2] *Sreyas Institute of Engineering& Technology, Hyderabad, India*
**Corresponding author E-mail: vharinadh@outlook.com*

Abstract

In the present analysis, thermo-mechanical process was employed to study the thermal and structural behaviour of three pass dissimilar butt-joints of SS316L to Inconel625 alloys. The temperatures evolution and residual stresses developed in the weldments were reported for each pass in the transverse direction to fusion zone. The Ansys Parametric Design Language (APDL) used for modelling and analysis of welding process with the double ellipsoidal heat source. The temperature dependent thermal and mechanical properties used in the simulation process. The residual stress is compressive in SS316L side compared to Inconel 625. The residual stress is within the yield limits of both base materials. The results obtained from the simulation process will be helpful for maintaining the structural integrity.

Keywords: *Dissimilar Materials; GTAW Multipass Welding; Heat Flux; FEA.*

1. Introduction

Fusion welding process is widely used for fabrication of the massive structure like ships, steel bridges etc., fusion process involves localised heating and cooling cycles in the base material. Inconel and stainless-steel combinations extensively used in nuclear reac- tors, aerospace, power plants, chemical industries etc., due to its high temperature and corrosion resistant. Goldak has proposed that the non-axis-symmetric 3-Dimensional heat source models for the welding simulations. The model suggested more realistic and has more flexible for heat sources for welding processes and the models used with for deep penetration of the weldments [1]. Dean Deng has reported that the welding simulation model for laser and GTAW processes with Gaussian and double ellipsoidal heat source model with constant and moving heat sources for understanding the temperatures, distortion and residual stresses in weldment of various joints for plate and pipe structures [2-3]. The 3-Dimensional model was developed for multipass dissimilar materials to understand the temperature distributions, distortion and residual stresses in the weldment using the ABAQUS packages [4]. Suresh and Harinadh have reported on various heat fluxes for joining similar and dissimilar butt joints for gas tungsten arc welding and laser beam welding process to understand the temperature distributions, distortion and residual stress developed in the process simulations for nuclear application materials [5-7]. Devendranath extensively discussed on the effect of filler wire on multipass dissimilar weldments of In- conel to SS and Monel to SS combinations are carried out using constant and pulsed current GTAW and made inference that the use of PCGTAW with ERNiCr-3 has resulted in better mechanical and microstructural properties while joining of dissimilar metals.
Naffakh has studied the relationship of weldability, microstructure and mechanical in dissimilar welding of SS310 to Inconel 657 [12-13]. A.G. Kamble has investigated the influence of welding input parameters on weld bead geometry, microstructure and mechanical properties for GMAW process and in his study includes the numerical model to understand the temperature distribution in transient condition and residual stress in the AISI321 steel using simulation package [14]. Vasantharaja has discussed residual stress and distortion for multipass TIG process and A-TIG welding process for 316LN thick plates [15]. The residual stresses reported for Tso-Liang Teng using FEA carries out steel plate with single-pass in arc welding process, this study includes the effect of travel speed in the weldment [16].
Inconel 625 superalloy and stainless steel 316L has extensively reported on microstructure, mechanical properties, and effect of various filler wires [18-19]. There was a gap in the literature to understand the impact of temperatures in the dissimilar multipass welding which leads to the generation of residual stress and distortions, and these lead to affect the efficiency of the joints in its cyclic operations. The multipass dissimilar welding simulation process is carried out with APDL. The transient thermal and static structure analysis is carried out for each pass. In this study, the temperatures and residual stresses are carried out for dissimilar combinations for SS316L to Iconel625. The thermo-mechanical simulation analysis is carried out using FEA, and the Fig-1 shows the detailed descrip- tion in the present process.

Copyright © 2018 Harinadh Vemanaboina et. al. This is an open access article distributed under the Creative Commons Attribution License, which permits unrestricted use, distribution, and reproduction in any medium, provided the original work is properly cited.

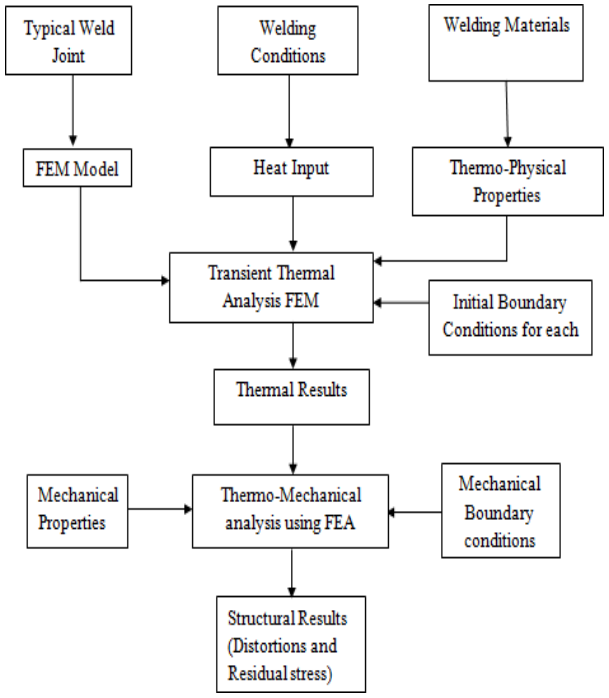


Fig. 1: Flowchart of the Sequentially Coupled Thermo-Mechanical Analysis Procedure.

2. Computational approach

The multipass dissimilar welding process used for the present study shown Fig. 2. The temperature dependents thermal and structural properties used for study as shown Fig. 3, for both stainless steel and Inconel plates. In multipass welding process, the material was filled at fusion zone pass by pass. The weld model dimensions are of 50 X 150 X 5 mm thick plate, the modelling and simulations were carried out with APDL language are shown in Fig. 5. The solid70 element used in the present simulations, the element supports both transient thermal analysis and structural analysis, the element changed to solid 45 in the structural analysis. The volumetric mesh used for the element with a size of 0.03 which used for both thermal and mechanical analysis as shown in Fig. 6. The thermo-mechanical welding simulation mainly depends upon the thermal and mechanical properties of the base material, welding conditions and techniques. The temperatures and residual stresses distribution are analysed for each pass. The Inter-pass temperature is maintained in between the passes to improve the metallurgical and mechanical properties and to control cracking occurring in the weldment. The American Welding Society (AWS) proposed the interpass temperature should not exceed 290^0C [17].

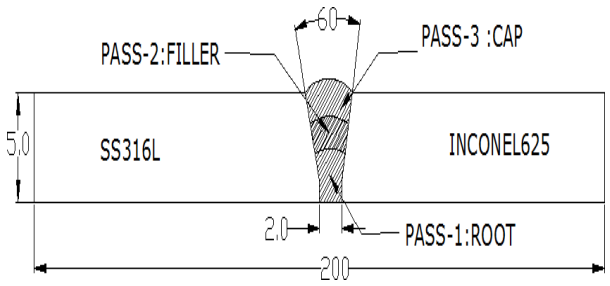


Fig. 2: Multipass-Welding Process.

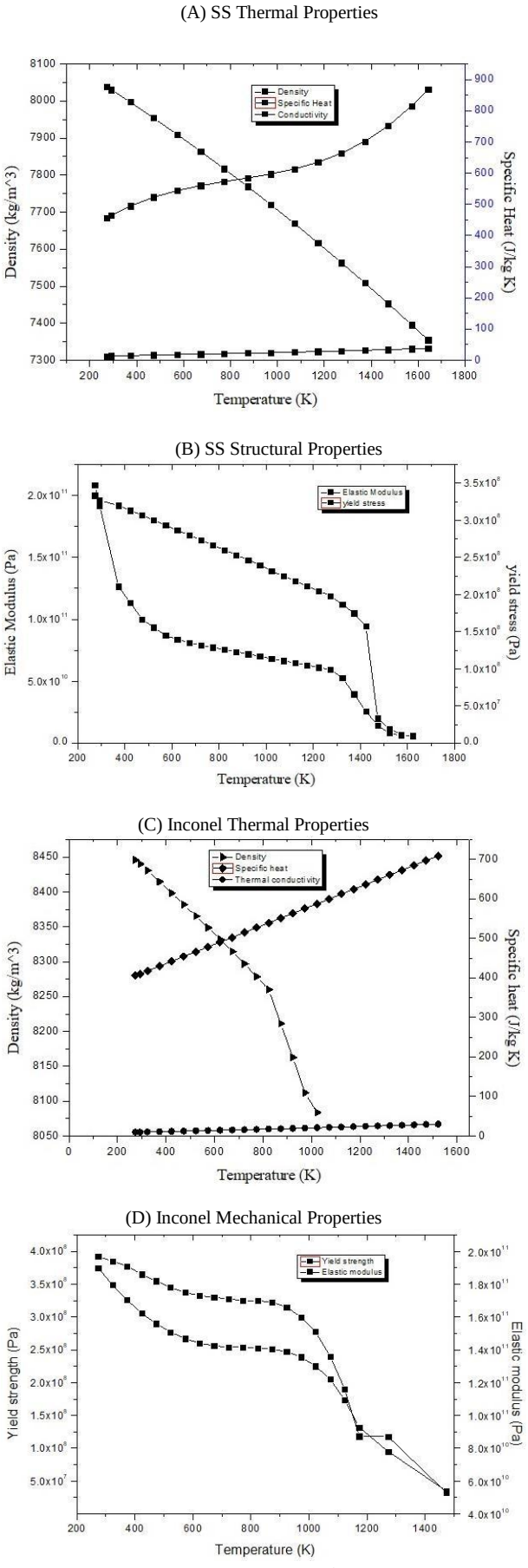


Fig. 3: Thermal and Mechanical Properties of SS and Inconel 625 Base Materials.

Heat source definition is essential for welding simulation in realistic models. The double ellipsoid [1] heat source was used for simulation analysis for GTAW processes as shown in Fig. 4. The left side and

right side of the model assign with SS316L to Inconel625 temperature dependent material properties (specific heat, density, thermal conductivity), the present simulation the model created using ANSYS package.

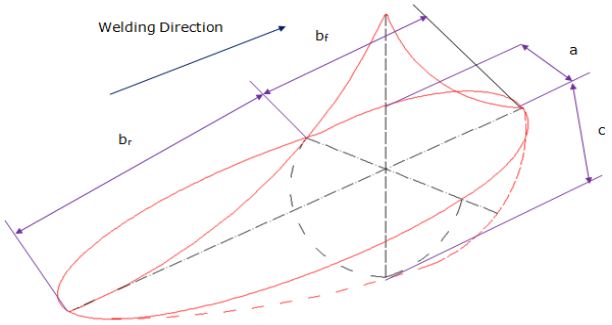


Fig. 4: Double Ellipsoidal Heat Flux.

The transient thermal problem in fusion welding processes involves heat conduction equation through suitable boundary conditions. The governing equation for quasi-steady state heat conduction is written as

$$\frac{\partial}{\partial x}\left(k\frac{\partial T}{\partial x}\right)+\frac{\partial}{\partial y}\left(k\frac{\partial T}{\partial y}\right)+\frac{\partial}{\partial z}\left(k\frac{\partial T}{\partial z}\right)+Q=-\rho C_p v\frac{\partial T}{\partial t} \quad (1)$$

Where ρ, C_p, k and T refers to material density, specific heat, thermal conductivity and time, v is the welding speed in along the Y-direction Q represents heat generation per unit time per unit volume.
The heat input to the model is calculated using the relation:

$$Q=\eta UI/V_H \quad (2)$$

Where η is the arc efficiency, U is the arc voltage, I is the welding current and V_H is the volumetric heat source. Heat input from the arc welding process can be modelled by a point source or a line source or as heat flux distributed on the surface and concentrated towards the center of the arc. Double ellipsoidal heat source model was adapted to calculate heat distribution for the processes as shown in Fig. 4.

Double ellipsoid, with a, b, c as semi-axes in 3 directions:

$$Q(x,y,z)=\frac{6\sqrt{3}r_f Q}{abc\pi\sqrt{\pi}}\exp\left(-\frac{3x^2}{c^2_{hf}}-\frac{3y^2}{a^2_h}-\frac{3z^2}{b^2_h}\right) \quad (3)$$

The combined convection and radiation boundary condition was used on the top surface, a combined heat transfer coefficient was calculated from the relationship where ε is the emissivity or degree of blackness of the surface of the body. A value of 0.7 was assumed for ε, as recommended for steel.

$$H = 24.1 * 10^{-4}\varepsilon T^{1.61} \quad (4)$$

The heat exchange between the welding and subsequent cooling takes place both by convection and radiation which are named as a dynamic boundary condition in heat transfer process. The boundary conditions of the process convection and radiation boundary condition are also take up for welding processes.

$$q_c=h(T-T_0) \quad (5)$$

$$q_r=\in\sigma(T^4-T_0^4) \quad (6)$$

Where T_0 is the ambient temperature; σ defined as the Stefan - Boltzmann constant; h and $\in$ are convection coefficient and emissivity, respectively.

2.1. Modelling

The simulation model developed for each pass by using APDL ANSYS package. In each pass, the thickness of weld bead added from 1.7 mm, for pass-2 and pass-3 the material was increased in the thickness along the plate from 1.7mm to 3.5mm and then 3.5mm to 5mm as shown in Fig .5.

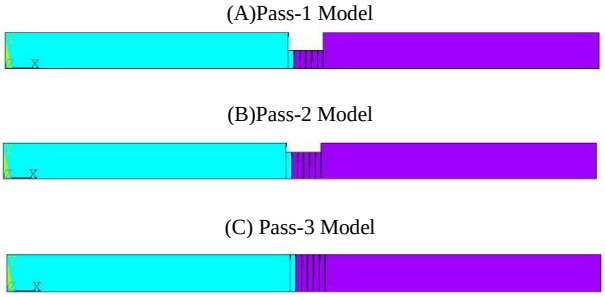


Fig. 5: Simulation Models for Each Pass.

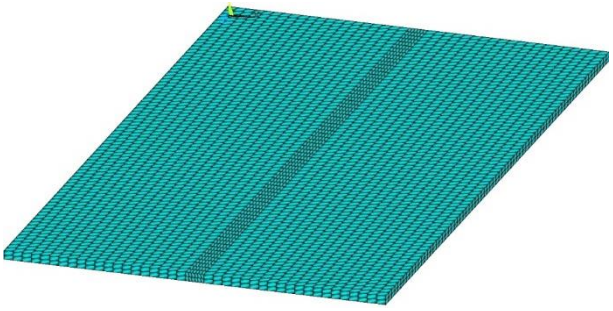


Fig. 6: Meshing of the Model.

2.2. Boundary conditions

1) The initial temperatures for pass-1 is the ambient temperature but in pass-2 and pass-3, the ambient temperature varies because of the heat absorbed from previous passes will be carried to further passes. The interpass temperatures between pass is maintained below 250^0C to avoid cracking in the materials due to heat.
2) In pass-1 the convection was applied on sides, bottom, top and root opening faces of the weldments, where there is no material in between root faces.
3) In pass-2 the convection was applied on sides, top and root opening faces and the root face decreased because where the material is filled with the weldments in the pass-1.
4) In pass-3, the convection was applied on sides, the top surface of the weldments.

3. Results and discussions

3.1. Temperature distribution

The transient thermal analysis was carried out for 40 sec for each pass, due to various thermal and mechanical properties of the base materials. The cooling cycle carried for 1000 sec, so the material come to ambient temperature. The maximum peak temperature is observed at the fusion zone. The heat was accumulated at the fusion zone of the weldment and spreads non-uniformly from weld centre to HAZ and further to all regions of the plate. The temperature distribution was widely spread along the SS plate because of high thermal conductivity of the material. The shorter temperature distribution was observed due

to low thermal and mechanical properties of the material. Fig. 7 shows the thermal profile of the weldments in the transverse direction for three passes. The arc at the mid-section of the plates has the sharp peak of the temperatures, and in cooling cycles, the plate reaches from ambient temperature 303 K to 1850 K in pass-1. The HAZ temperature on both sides of the weldments was around 1150 K. The base plate temperatures were recorded around 300 K. In the pass-2, the Interpass temperature was ended temperature of pass-1, and it was reported to be 303 K, and at fusion zone the temperature of 1800 K reported, and it decreased to 380 K when it moves to the end of the plate. The Inter-pass temperature for pass-3 was at 350 K, the temperature rises to 1700 K at the fusion zone and the end of the simulation the edges reached to 410 K. Among the thermal profiles in the entire passes, the SS316L experienced high temperatures compared to Inconel.

3.2. Residual stress

The residual stresses are measured at cut section of the thickness of the plate at a distance 1.5 mm from the bottom surface. The stress distributions of the weldment are shown in the Fig. 8 for pass-1. The observed distributions are caused due to thermal expansion and contraction between the plates. It has been observed that the Inconel 625 has to experience tensile stresses when compared with the SS316L side. This behaviour may be attributed to the difference in thermal conductivity and thermal expansion of both the metal alloys can be observed from the Fig. 3.

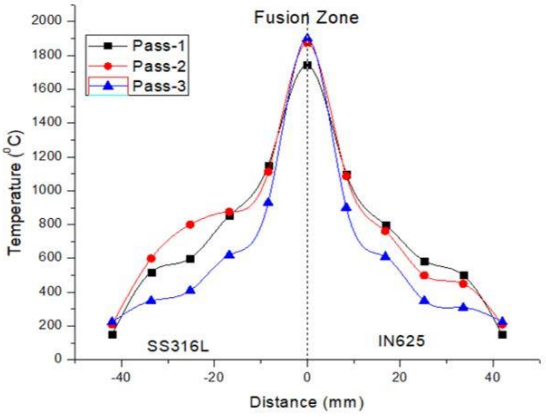


Fig. 7: Temperature Distribution in the Weldment

It has been observed that the SS metal has high thermal conductivity as compared to Inconel, which tends the SS to contract more during solidification which results in generation or development of compressive stress. Whereas, in Inconel side was higher resistant material and low thermal conduction value, resulting production less in stresses as compared to SS side.

Fig. 9 shows the residual stress distribution in pass-2. It was observed that weld zone was experiencing compressive stress as compared to HAZ regions in the weldment. This behaviour was attributed due to maintenance of inter-pass temperature or may be due to the phase change.

The residual stress distribution of the pass-3 as shown in Fig. 10. It has been observed that the weld region results in the high tensile stresses. Due to the expansion of the metal plates as cumulative heat flux is added from the Interpass temperature. To compensate the compressive loads in the HAZ regions, on both sides of the plates. The residual stresses are self-balanced in the weldment and within yield limits of the materials after the welding process

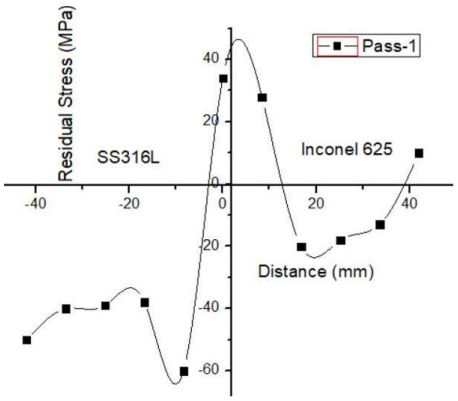


Fig. 8: Residual Stress in Pass-1.

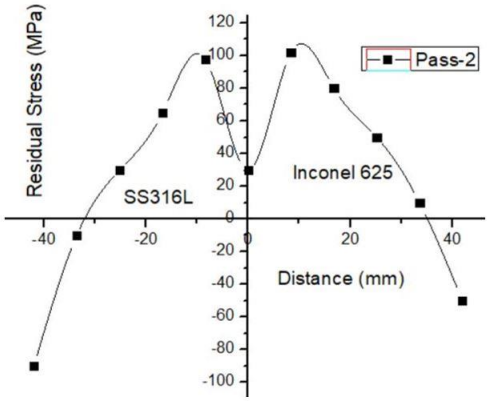


Fig. 9: Residual Stresses in Pass-2.

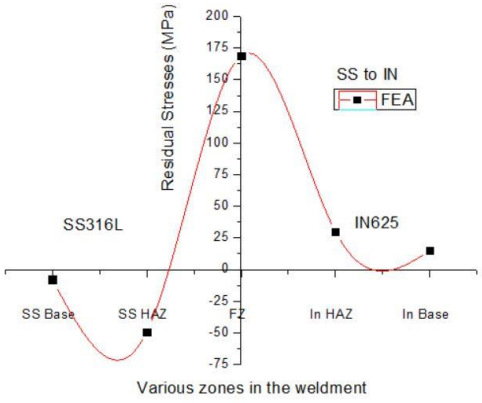


Fig. 10: Residual Stresses in Pass-3.

4. Conclusion

In this work, the residual stress was observed within the yield limit of the materials. The temperatures were reported to be high at SS side comparative to Inconel material due to variation in thermal and mechanical properties of the base materials. The tensile and compressive stress generated through various thermal cycles were self-balanced within the structure.

- The temperatures in the pass-1 was observed to be 1800 K. The temperatures at pass-2 and pass-3 were 1910 K and 1780 K respectively.
- The residual stresses in pass-1 are in tension at Inconel of 34 MPa at HAZ, and remaining plates were in compressive both sides of the plate to maintain force balance.
- The residual stress in pass-2 for both the fusion zone and HAZ is in the tension of 27 MPa and 102 MPa and base material ending with compressive residual stresses.

- In pass-3 residual stresses at the fusion zone was 169 MPa and SS HAZ was compressive, and Inconel HAZ is in tension stresses.
- The residual stresses were self-balanced within the weld structure in pass-3 after the two passes, where both ends of the base plates are ending with compressive stresses in the base plate.
- The factor of safety of 1.25. The residual stresses is self-balanced and within the yield limits of materials.

References

[1] Goldak J, Chakravariti A,Bibby M (1984).Anew finiteelement model for welding heatsources. Metall Trans B, 1411–6.

[2] Deng, Dean, Hidekazu Murakawa, and Wei Liang (2008). "Numerical and Experimental Investigations on Welding Residual Stress in Multi-Pass Butt-Welded Austenitic Stainless Steel Pipe." Computational Materials Science 42.2, 234–244. https://doi.org/10.1016/j.commatsci.2007.07.009.

[3] Deng, D., Murakawa, H., (2006). Prediction of welding residual stress in multi-pass butt-welded modified 9Cr–1Mo steel pipe considering phase transformation effects. Computational Materials Science 37, 209–219. https://doi.org/10.1016/j.commatsci.2005.06.010.

[4] A. Capriccioli and P. Frosi(2009). "Multipurpose ANSYS FE procedure for welding processes simulation," Fusion Engineering and Design, 84 (2–6). 546–553. https://doi.org/10.1016/j.fusengdes.2009.01.039.

[5] S. Akella, H. Vemanaboina, and R. Kumar Buddu (2016). "Heat Flux for Welding Processes: Model for Laser Weld," Sreyas International Journal of Scientists and Technocrats, 1(1), 10–15. https://doi.org/10.24951/sreyasijst.org/2016011002.

[6] H. Vemanaboina, S. Akella, and R. K. Buddu (2014). "Welding Process Simulation Model for Temperature and Residual Stress Analysis," Procedia Materials Science, 6, 1539–1546. https://doi.org/10.1016/j.mspro.2014.07.135.

[7] M. S. Akella, M. V. Harinadh, M. Y. Krishna, and M. R. K. Buddu (2014). "A Welding Simulation of Dissimilar Materials SS304 and Copper," Procedia Materials Science, 5, 2440–2449. https://doi.org/10.1016/j.mspro.2014.07.490.

[8] Ramkumar, Kasinath Devendranath et al (2014). "Characterization of Microstructure and Mechanical Properties of Inconel 625 and AISI 304 Dissimilar Weldments." ISIJ International 54 (4) 900–908. https://doi.org/10.2355/isijinternational.54.900.

[9] Kumar, K. Gokul, K. Devendranath Ramkumar, and N. Arivazhagan(2015). "Characterization of Metallurgical and Mechanical Properties on the Multi-Pass Welding of Inconel 625 and AISI 316L." Journal of Mechanical Science and Technology 29 (3), 39–1047. https://doi.org/10.1007/s12206-014-1112-4.

[10] K. Devendranath Ramkumar, N. Arivazhagan, and S. Narayanan (2012). "Effect of filler materials on the performance of gas tungsten arc welded AISI 304 and Monel 400," Materials & Design, 40. 70–79. https://doi.org/10.1016/j.matdes.2012.03.024.

[11] P. Mithilesh, D. Varun, A. R. G. Reddy, K. D. Ramkumar, N. Arivazhagan, and S. Narayanan(2014). "Investigations on Dissimilar Weldments of Inconel 625 and AISI 304," Procedia Engineering, 75, 66–70. https://doi.org/10.1016/j.proeng.2013.11.013.

[12] Naffakh, H., M. Shamanian, and F. Ashrafizadeh(2008). "Weldability in Dissimilar Welds between Type 310 Austenitic Stainless Steel and Alloy 657." Journal of Materials Science 43 (15) 5300–5304. https://doi.org/10.1007/s10853-008-2761-4.

[13] Naffakh, H., M. Shamanian, and F. Ashrafizadeh(2008). "Influence of Artificial Aging on Microstructure and Mechanical Properties of Dissimilar Welds between 310 Stainless Steel and INCONEL 657." Metallurgical and Materials Transactions A 39(10)2403–2415. https://doi.org/10.1007/s11661-008-9598-y.

[14] A. G. Kamble and R. V. Rao (2013). "Experimental investigation on the effects of process parameters of GMAW and transient thermal analysis of AISI321 steel," Advances in Manufacturing, 1 (4), 362–377. https://doi.org/10.1007/s40436-013-0041-2.

[15] P. Vasantharaja, V. Maduarimuthu, M. Vasudevan, and P. Palanichamy (2012). "Assessment of Residual Stresses and Distortion in Stainless Steel Weld Joints," Materials and Manufacturing Processes, 27, (12), 1376–1381. https://doi.org/10.1080/10426914.2012.663135.

[16] T.-L. Teng and C.-C. Lin (1998). "Effect of welding conditions on residual stresses due to butt welds," International Journal of Pressure Vessels and Piping, 75, (12), 857–864. https://doi.org/10.1016/S0308-0161(98)00084-2.

[17] The Importance of Interpass Temperature Welding Innovation Vol. XV, No. 1, 1998.

[18] C.H Muralimohan, S. Haribabu, Y. Hariprasada Reddy, V. Muthupandi, K. Sivaprasad (2015). "Joining of AISI 1040 Steel to 6082-T6 Aluminium Alloy by Friction Welding, "Journal of Advances in Mechanical Engineering and Science, 1, (1), 57-64. https://doi.org/10.18831/james.in/2015011006.

[19] V. Saravenan, S. Rajakumar, A. Muruganandam (2016). "Influence of tool rotation speed on macrostructure, microstructure and mechanical behaviour of dissimilar friction stir welded AA2014-T6 and AA7075-T6 Aluminium alloys," Journal of Advances in Mechanical Engineering and Science, 2, (4), 19-24. https://doi.org/10.18831/james.in/2016041003.